Performance Analysis of GNSS + 5G Hybrid Positioning Algorithms for Smartphones in Urban Environments

Qi Liu, Chengfa Gao, Alda Xhafa, Wang Gao, José A. López-Salcedo, *Senior Member, IEEE*, and Gonzalo Seco-Granados, *Fellow, IEEE*

***Abstract*— Smartphone positioning methods relying solely on global navigation satellite system (GNSS) are susceptible to significant errors in urban environments due to challenging observation conditions. To enhance position accuracy, this article introduces a novel fifth-generation (5G) observation model based on unit vectors and evaluates its performance using several user locations and precision observation data. The results demonstrate that the unit vector method, compared to the traditional angle of departure (AOD) approach, effectively reduces the nonlinearity of the observation model, leading to a substantial improvement in the 5G system's positioning accuracy. Furthermore, we conduct experiments to investigate the impact of the geometric distribution of 5G base station (BS) height on positioning accuracy. The results reveal a significant influence, highlighting the importance of considering BS height in the positioning process. In the urban environment, introducing 5G BS angle observations as an aid to GNSS significantly enhances the reliability of smartphone positioning, achieving positioning errors of less than one meter. Notably, this approach outperforms the introduction of 5G distance observations, providing valuable insights for the development of seamless indoor and outdoor positioning systems in the future.**

***Index Terms*— Fifth-generation (5G), global navigation satellite system (GNSS), hybrid positioning, smartphone, unit vector.**

I. Introduction

LOCATION-BASED services play a crucial role in various applications such as smart cities and autonomous driving [1], [2]. Among equipments of mobile location-based services, smartphones have garnered significant attention from researchers [3], [4]. While global navigation satellite systems (GNSS) can provide accurate position, speed, and time solutions in open outdoor environments [5], [6], [7], their performance is hampered in urban settings due to weaker satellite signals, resulting in lower data quality [8], [9]. Indeed, GNSS alone cannot achieve high-precision positioning in these occluded scenarios.

To address this limitation, the fifth-generation mobile communication technology (5G) offers promising solutions for position estimation in urban environments [10]. Specifically, 5G millimeter wave (mm-wave) technology, with its larger bandwidth and higher frequency compared to 4G, effectively suppresses multipath interference. Additionally, 5G employs large-scale antenna arrays, enhancing angle and distance estimation performance [11]. Currently, 5G networks play an important role in the construction of smart cities [12] and can help cities reduce energy consumption and environmental pollution [13]. Furthermore through the 5G network system to achieve traffic flow optimization and energy management, countries can better achieve the goals of sustainable development [14].

Researchers are exploring additional techniques and devices to aid GNSS positioning in urban areas. For instance, a Bluetooth network can achieve a positioning accuracy of approximately 2 meters in outdoor environments [15]. Ultra-wideband (UWB) technology, known for its strong penetrating power and antiinterference capabilities, provides supplementary observations for GNSS in urban settings, enabling decimeter-level positioning accuracy during motion [16]. Moreover, the combination of GNSS and WI-FI reference signal strength index (RSSI) fingerprint technology improves the reliability of mobile phone navigation solutions in certain occlusion environments [17]. However, the cost and limited usability of external devices make them less favorable options for smartphone positioning. In contrast, 5G mm-wave leverages existing communication base stations (BSs) without the need for additional equipment, offering a cost-effective advantage. Similarly, researchers use methods like inertial navigation system (INS) [18] and pedestrian dead reckoning (PDR) [19] to maintain positioning continuity and reliability without external equipment, although error accumulation remains a challenge.

The 5G signal provides observations for different positioning methods, summarized in Table I. Current 5G positioning method are divided into three categories: 1) time-based method like time of arrival (TOA), time difference of arrival (TDOA) [20], and round-trip time (RTT) [21]; 2) angle-based method, including angle of departure (AOD), angle of arrival (AOA); and 3) a combinations of these approaches [22], [23], [24]. The 5G system's cost-effectiveness allows for decimeter-level or even centimeter-level positioning accuracy, facilitating improved GNSS reliability in specific environments, attracting special attention from researchers.

Manuscript received 8 August 2023; revised 30 October 2023; accepted 13 November 2023. Date of publication 1 December 2023; date of current version 29 December 2023. This work was supported in part by the National Key Research and Development Program of China under Grant 2021YFC3000502, in part by the China Scholarship Council under Grant 202206090175, and in part by the Natural Science Foundation of Jiangsu Province under Grant BK20221475. The Associate Editor coordinating the review process was Dr. Nuria Novas. *(Corresponding author: Chengfa Gao.)*

Qi Liu is with the Department of Transportation, Southeast University, Nanjing, Jiangsu 211189, China, and also with the Department of Telecommunications and Systems Engineering, Universitat Autònoma de Barcelona (UAB), Bellaterra, 08193 Barcelona, Spain.

Chengfa Gao is with the Department of Transportation, Southeast University, Nanjing, Jiangsu 211189, China (e-mail: gaochfa@163.com).

Alda Xhafa, José A. López-Salcedo, and Gonzalo Seco-Granados are with the Department of Telecommunications and Systems Engineering, Universitat Autònoma de Barcelona (UAB), Bellaterra, 08193 Barcelona, Spain.

Wang Gao is with the Department of Instrument Science and Engineering, Southeast University, Nanjing, Jiangsu 211189, China.

Digital Object Identifier 10.1109/TIM.2023.3338677

1557-9662 © 2023 IEEE. Personal use is permitted, but republication/redistribution requires IEEE permission.
See https://www.ieee.org/publications/rights/index.html for more information.
Authorized licensed use limited to: Universitat Autonoma De Barcelona. Downloaded on January 18,2024 at 17:09:47 UTC from IEEE Xplore. Restrictions apply.

TABLE I
COMPARISON AND ANALYSIS OF 5G AND GNSS POSITIONING METHODS

System	5G		GNSS	GNSS+5G
Parameter	Time-based observations: transmission time from BS to UE	Angle-based observations: azimuth and elevation angles	Pseudorange and carrier	GNSS observations + 5G observations
Method	TOA, TDOA ,RTT	AOA, AOD	RTK, PPP	GNSS+ 5G-TDOA [25] GNSS + 5G-TOA and received signal strength [26]
Performance	Large bandwidth suppresses multipath; Higher ranging accuracy; Maintain line of sight between BS and UE		Excellent satellite visibility and number of satellites; Great coverage; At least four satellites.	Assisted GNSS positioning; More observations; More accurate navigation solutions in urban environments.
Disadvantages	Clock synchronization error; High complexity [27], [28]; Hardware delays [29].	High hardware requirements; Energy consumption; Small coverage [30].	Poor stability; Affected by the environment; Poor anti-interference.	For applications such as autonomous driving, GNSS + 5G time-based observations cannot meet the accuracy requirements.

Smartphone positioning is affected by insufficient satellite visibility in urban environment. The introduction of 5G TOA can improve this situation, and positioning performance is significantly enhanced after optimizing the configuration of 5G BSs [25]. In the GNSS/5G integrated system, the joint use of 5G TOA and received signal strength measurements can significantly decrease positioning position deviations [26]. Combining the RTT observations of 5G signals with GNSS observations through distance observation abstraction can significantly enhance the positioning accuracy and availability of GNSS navigation solutions [27]. Furthermore, 3D maps help analyze satellite and BS visibility, reducing nonline-of-sight satellite interference and enhancing positioning accuracy [28]. Optimizing the planar geometric configuration of 5G BSs further improves the performance of hybrid positioning systems [29]. Nevertheless, relying solely on distance observation may not suffice for scenarios like autonomous driving. Some works have introduced AOA observations into the GNSS and 5G fusion positioning model to compensate for the lack of GNSS visibility in urban environments [30]. However, the challenge lies in maintaining a stable orientation of the mobile device, which can impact system performance. Reducing the linearization error of the 5G positioning system is equally crucial for enhancing positioning accuracy.

Based on the above analysis, this study proposes a new 5G observation model to reduce the linearization errors. Subsequently, we construct a GNSS and 5G hybrid positioning model to further improve smartphone positioning accuracy in urban environments, which we validate through experiments. The structure of this article is organized as follows: Section II introduces the GNSS and 5G observation model, Section III explains the proposed hybrid GNSS + 5G positioning algorithm and evaluates the performance of the proposed model through experiments. Finally, Section IV presents the conclusions.

II. METHODOLOGY

This section describes the distance-based and angle-based traditional observation models for 5G positioning, as well as the GNSS observation models. To reduce the nonlinearity of the 5G observation equation, we introduce the observation model based on the unit vectors and derive the form of its covariance matrix. Finally, the fusion positioning model of GNSS and 5G is constructed.

A. 5G Observations Model

As shown in Fig. 1, a 5G positioning system consists of several BSs and a user equipment (UE). Locations of the BSs and UE are denoted by $R_{\mathrm{BS},i} = [x_i, y_i, z_i](i = 1, 2, 3, \ldots, n)$ and $R_{\mathrm{UE}} = [x, y, z]$, n is the number of the BSs. For 5G system, there are two commonly used types of observations: distance d and angle α, θ.

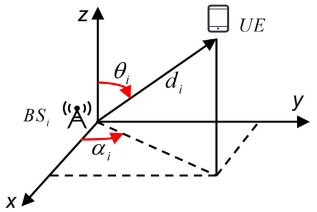

Fig. 1. Transmission links and geometry of the scenario including the 5G BSs at location $R_{\mathrm{BS},i}$ and UE at location R_{UE}. The angle α and θ are the azimuth and elevation.

1) TOA Observations Model: For the TOA of 5G measurements, the following observation model will be used [31]:

$$P_{5\mathrm{G},i} = d_i + c \cdot dt_{i,ue} + \epsilon_i \tag{1}$$

where the $P_{5\mathrm{G},i}$ is the distance observation, $d_i = ((x_i - x)^2 + (y_i - y)^2 + (z_i - z)^2)^{1/2}$ is the geometric distance between the BS_i and UE. c is the speed of light, dt is the clock offset between the BSs and the UE, and the ϵ represents the noise.

2) AOD Observations Model: In the angle-based method, the observation $z = [\theta_i \ \alpha_i]^T$ of AOD can be expressed as follows:

$$\begin{cases} \theta_i = \arccos\dfrac{(z - z_i)}{d_i} \\ \alpha_i = \arctan\dfrac{(y - y_i)}{(x - x_i)} \end{cases} \tag{2}$$

where θ is the elevation and α is the azimuth. The corresponding transition matrix $\mathbf{H_{AOD}}$, which is used in the linearization process, can be written as follows:

$$\begin{aligned} \mathbf{H_{AOD}} &= \begin{bmatrix} \dfrac{\partial \alpha_i}{\partial x} & \dfrac{\partial \alpha_i}{\partial y} & \dfrac{\partial \alpha_i}{\partial z} \\ \dfrac{\partial \theta_i}{\partial x} & \dfrac{\partial \theta_i}{\partial y} & \dfrac{\partial \theta_i}{\partial z} \end{bmatrix} \\ &= \begin{bmatrix} \dfrac{-(y - y_i)}{l_i^2} & \dfrac{(x - x_i)}{l_i^2} & 0 \\ \dfrac{(z - z_i)(x - x_i)}{l_i d_i^2} & \dfrac{(z - z_i)(y - y_i)}{l_i d_i^2} & \dfrac{-l_i}{d_i^2} \end{bmatrix} \end{aligned} \tag{3}$$

where $l_i = ((x - x_i)^2 + (y - y_i)^2)^{1/2}$, and the weight matrix $\mathbf{W_{AOD}} = \mathrm{diag}[\sigma_{\alpha,1}^2 \ \sigma_{\theta,1}^2 \ \cdots \ \sigma_{\alpha,n}^2 \ \sigma_{\theta,n}^2]^{-1}$.

Authorized licensed use limited to: Universitat Autonoma De Barcelona. Downloaded on January 18,2024 at 17:09:47 UTC from IEEE Xplore. Restrictions apply.

For GNSS, the distance between the satellite and the receiver reaches tens of thousands of kilometers, the linearization errors can be ignored, while for 5G system, the impact of linearization error cannot be ignored. Therefore, to reduce the nonlinear degree of 5G observation equation, we introduce the unit vector observation model based on the geometric relationship between the BSs and UE.

3) Unit Vector Observations Model: From Fig. 1, it can be observed that the positional relationship between BS and the UE is as follows:

$$\begin{cases} R_{\mathrm{UE}} = R_{\mathrm{BS},i} + ||R_{\mathrm{BS},i} - R_{\mathrm{UE}}|| \cdot u_i \\ u_i = \begin{bmatrix} \cos(\alpha_i)\sin(\theta_i) \\ \sin(\alpha_i)\sin(\theta_i) \\ \cos(\theta_i) \end{bmatrix} \end{cases} \tag{4}$$

where u_i represents the unit vector, R_{UE} and $R_{\mathrm{BS},i}$ represent the UE location and BS location, respectively, and the subscript i indicates the BS identification number. It can be clearly seen that the degree of nonlinearity of the unit vector model is lower than that of the traditional AOD observation equation. The corresponding transition matrix of unit vector $\mathbf{H_{UV}}$ can be expressed as follows:

$$\mathbf{H_{UV}} = \begin{bmatrix} \frac{\partial R_{\mathrm{UE},x}}{\partial x} & \frac{\partial R_{\mathrm{UE},x}}{\partial y} & \frac{\partial R_{\mathrm{UE},x}}{\partial z} \\ \frac{\partial R_{\mathrm{UE},y}}{\partial x} & \frac{\partial R_{\mathrm{UE},y}}{\partial y} & \frac{\partial R_{\mathrm{UE},y}}{\partial z} \\ \frac{\partial R_{\mathrm{UE},z}}{\partial x} & \frac{\partial R_{\mathrm{UE},z}}{\partial y} & \frac{\partial R_{\mathrm{UE},z}}{\partial z} \end{bmatrix} \tag{5}$$

where

$$\begin{cases} \frac{\partial R_{\mathrm{UE},x}}{\partial x} = 1 - \sin(\theta_i)\cos(\alpha_i)\frac{(x - x_i)}{||R_{\mathrm{BS},i} - R_{\mathrm{UE}}||} \\ \frac{\partial R_{\mathrm{UE},x}}{\partial y} = \frac{-(y - y_i)}{||R_{\mathrm{BS},i} - R_{\mathrm{UE}}||}\sin(\theta_i)\cos(\alpha_i) \\ \frac{\partial R_{\mathrm{UE},x}}{\partial z} = \frac{-(z - z_i)}{||R_{\mathrm{BS},i} - R_{\mathrm{UE}}||}\sin(\theta_i)\cos(\alpha_i) \\ \frac{\partial R_{\mathrm{UE},y}}{\partial x} = \frac{-(x - x_i)}{||R_{\mathrm{BS},i} - R_{\mathrm{UE}}||}\sin(\theta_i)\sin(\alpha_i) \\ \frac{\partial R_{\mathrm{UE},y}}{\partial y} = 1 - \sin(\theta_i)\sin(\alpha_i)\frac{(y - y_i)}{||R_{\mathrm{BS},i} - R_{\mathrm{UE}}||} \\ \frac{\partial R_{\mathrm{UE},y}}{\partial z} = \frac{-(z - z_i)}{||R_{\mathrm{BS},i} - R_{\mathrm{UE}}||}\sin(\theta_i)\sin(\alpha_i) \\ \frac{\partial R_{\mathrm{UE},z}}{\partial x} = \frac{-(x - x_i)}{||R_{\mathrm{BS},i} - R_{\mathrm{UE}}||}\cos(\theta_i) \\ \frac{\partial R_{\mathrm{UE},z}}{\partial y} = \frac{-(y - y_i)}{||R_{\mathrm{BS},i} - R_{\mathrm{UE}}||}\cos(\theta_i) \\ \frac{\partial R_{\mathrm{UE},z}}{\partial z} = 1 - \cos(\theta_i)\frac{(z - z_i)}{||R_{\mathrm{BS},i} - R_{\mathrm{UE}}||}. \end{cases} \tag{6}$$

R_{UE}, $R_{\mathrm{BS},i}$ represent the UE location and BS location, respectively, and the subscript x, y, and z indicate the coordinates in the three directions of east, north, and up. In the unit vector model, the observations are not completely independent, so the weight matrix needs to be redesigned. The weight matrix for unit vector method $\mathbf{W_{uv}}$ is as follows:

$$\mathbf{W_{uv}} = \begin{bmatrix} D_{xx} & D_{xy} & D_{xz} \\ D_{yx} & D_{yy} & D_{yz} \\ D_{zx} & D_{zy} & D_{zz} \end{bmatrix} \tag{7}$$

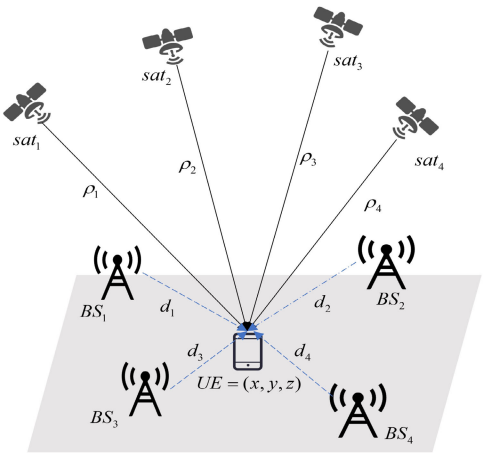

Fig. 2. System model of GNSS and 5G hybrid positioning.

where D_{xx}, D_{yy}, and D_{zz} are the variance of the observation and D_{xy}, D_{xz}, and D_{yz} are the covariance between observations. The variance and covariance can be modeled by

$$\begin{cases} D_{xx} = \sin^2\alpha_i\sin^2\theta_i\sigma_\alpha^2 \\ \qquad + \sin^2\alpha_i\cos^2\theta_i\sigma_\alpha^2\sigma_\theta^2 + \cos^2\alpha_i\cos^2\theta_i\sigma_\theta^2 \\ D_{yy} = \sin^2\theta_i\cos^2\alpha_i\sigma_\alpha^2 \\ \qquad + \cos^2\alpha_i\cos^2\theta_i\sigma_\alpha^2\sigma_\theta^2 + \sin^2\alpha_i\cos^2\theta_i\sigma_\theta^2 \\ D_{zz} = \sin^2\theta_i\sigma_\theta^2 \\ D_{xy} = D_{yx} = -\sin^2\theta_i\sin\alpha_i\cos\alpha_i\sigma_\alpha^2 \\ \qquad - \cos^2\theta_i\sin\alpha_i\cos\alpha_i\sigma_\alpha^2\sigma_\theta^2 \\ \qquad + \cos^2\theta_i\sin\alpha_i\cos\alpha_i\sigma_\theta^2 \\ D_{xz} = D_{zx} = -\sin\theta_i\cos\theta_i\cos\alpha_i\sigma_\theta^2 \\ D_{yz} = D_{zy} = \sin\theta_i\cos\theta_i\sin\alpha_i\sigma_\theta^2 \end{cases} \tag{8}$$

where θ is the elevation and α is the azimuth. i represents the BS number and σ represents the standard deviation of observations.

B. GNSS Observations Model

The GNSS observations of the satellite s tracked by receiver r can be expressed as follows:

$$P_s = \rho_s + c(dt_r - dt_s) + I + T + e_s \tag{9}$$

where $\rho = ((x_{s,i} - x)^2 + (y_{s,i} - y)^2 + (z_{s,i} - z)^2)^{1/2}$ is the geometric distance between the satellite and the receiver, and the subscripts s, r represent satellite and receiver, respectively. P represents the pseudorange. c is the light speed and dt is the clock error. I, T represent the ionospheric delay error and the tropospheric delay error. e is the pseudorange noise. And the weight of the satellite is determined by taking into account the carrier-to-noise ratio (C/N_0), as follows [32]:

$$\sigma_s^2 = a \cdot 10^{-(C/N_0)/10} + b \tag{10}$$

where a and b are the constants.

C. GNSS + 5G Hybrid Observation Model

The schematic of the hybrid positioning system is shown in Fig. 2. We assume that M satellites and N BSs can be

Authorized licensed use limited to: Universitat Autonoma De Barcelona. Downloaded on January 18,2024 at 17:09:47 UTC from IEEE Xplore. Restrictions apply.

observed in each epoch for hybrid system, convert the above GNSS and 5G observation models into a unified coordinates system, and use (4) and (9) to construct the GNSS + 5G hybrid positioning observation equation

$$\begin{cases} P_1 = \rho_1 + c(dt_r - dt_1) + I + T + e_1 \\ P_2 = \rho_2 + c(dt_r - dt_2) + I + T + e_2 \\ \quad \vdots \\ P_m = \rho_3 + c(dt_r - dt_m) + I + T + e_m \\ R_{\mathrm{UE},1} = R_{\mathrm{BS},1} + ||R_{\mathrm{BS},1} - R_{\mathrm{UE}}|| \cdot u_1 \\ \quad \vdots \\ R_{\mathrm{UE},n} = R_{\mathrm{BS},n} + ||R_{\mathrm{BS},n} - R_{\mathrm{UE}}|| \cdot u_n \end{cases} \tag{11}$$

where m is the number of satellite and n is the number of BS. We use the intersatellite single difference to eliminate the UE clock error, and use the clock file and correction model to correct the satellite clock error, ionosphere and troposphere delay. The weight least squares (WLSs) algorithm is used to solve the unknown parameters, and it can be constructed as follows [33]:

$$Z = G(X) + V \tag{12}$$

where Z is the observation, $X = [x\ y\ z]^T$ is the state vector, $G(X)$ is the modeled observation, and V is the residual of the observation. We can obtain the linearized error equation by applying Taylor's first-order expansion at the initial value X_0, as follows:

$$V = -\mathbf{H} \cdot dX + L \tag{13}$$

where $\mathbf{H}$ is a coefficient matrix consisting of the partial derivatives of the observation equation with respect to the parameters. $L = Z - G(X_0)$ is the difference between the observed value and the modeled observation, and $dX = [\Delta x\ \Delta y\ \Delta z]^T$ is the correction for the unknown parameters to be calculated. The solution for the hybrid system can be produced by using an iterative solution approach.

$$\begin{aligned} X &= X_0 + dX \\ dX &= (\mathbf{H^T W H})^{-1}\mathbf{H^T W} L \end{aligned} \tag{14}$$

where X_0 is the solution of the previous epoch and the meanings of the remaining parameters are the same as (13) and (14). In the first epoch, it can be represented by the approximate coordinates of UE. And $\mathbf{W}$ is the weight matrix for the hybrid observation model, which can be expressed as follows:

$$\mathbf{W} = \begin{bmatrix} \frac{1}{\sigma_{s,1}^2} & & & & \\ & \ddots & & & \\ & & \frac{1}{\sigma_{s,m}^2} & & \\ & & & (\mathbf{H_{uv,1}})_{3\times3}^{-1} & \\ & & & & \ddots \\ & & & & (\mathbf{H_{uv,n}})_{3\times3}^{-1} \end{bmatrix}_{(m+n)\times(m+n)}. \tag{15}$$

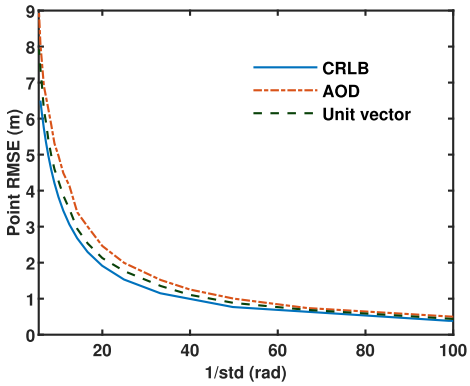

Fig. 3. Comparison of different point accuracy of AOD/Unit vector/CRLB.

III. Simulation Results

This section first compares the effects of the two 5G models using several user locations and precision observation data. Additionally, we experimentally investigate the influence of the geometric distribution of BS's heights on localization performance. The convergence probabilities of these models are subsequently assessed, taking into account the initial coordinate deviations. Finally, introducing 5G BS angle observations as an aid to GNSS and evaluating the performance of the hybrid model.

A. 5G Simulation Experiment

1) For Cramer–Rao Bound: In practical implementation, the TOA method requires strict time synchronization between 5G BSs and UE, leading to elevated deployment costs, whereas the angle-based positioning method can avoid these errors. Therefore, we use the angle-based method for subsequent 5G positioning research. We deploy BSs in this research based on the simulation method of outdoor environment within 5G positioning research in 3GPP Release 16 [34]. To qualitatively compare the performance of the AOD and the proposed unit vector method, we added a bias between 0° to 10° to the angular observations in the simulation and analyze the theoretical bound Cramer–Rao lower bound (CRLB) [35].

CRLB gives a lower bound on the variance achievable with any unbiased estimate using the same data, so it can serve as an important benchmark against which to compare the performance of localization algorithms. It can be seen from Fig. 3 that the increasing standard deviation (std) of the 5G dataset' observation noise leads to an increase in the positioning point error of the AOD method, while the unit vector method can still provide an accurate solution.

2) For Empirical 3-D Position Error: To quantitatively analyze the performance of the two methods, we simulate four sets of 5G observation data, the mean value of the observation noise is set to equal 0, and the stds are set to be 0.5°, 1°, 1.5°, and 2°. Table II shows the location of each BS in the simulation experiment, the coordinate of UE is (0, 0, 0). The height of some 5G BSs is higher than the one of UE, while it is lower for other BSs, so to provide a reasonable geometric configuration for the 5G system.

Fig. 4 presents the 3-D positioning errors of the simulated data under distinct accuracy conditions for BSs deployment scenarios detailed in Table II. It can be seen that both methods

Authorized licensed use limited to: Universitat Autonoma De Barcelona. Downloaded on January 18,2024 at 17:09:47 UTC from IEEE Xplore. Restrictions apply.

TABLE II
COORDINATES OF BSS

Base stations	X	Y	Z
1	95.553	94.863	30.005
2	-65.064	96.594	-22.122
3	-64.137	-104.157	24.283
4	98.295	-103.662	-26.292

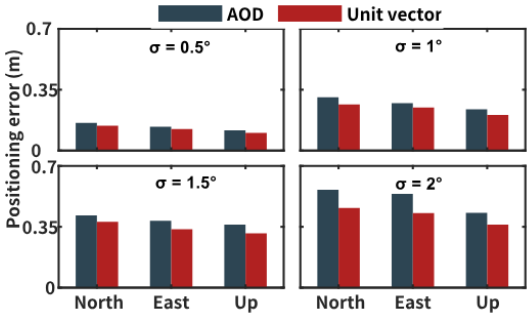

Fig. 4. 5G positioning result of AOD/Unit vector.

TABLE III
COORDINATES OF BSS. THE HEIGHT OF BS IS HIGHER THAN THAT OF UE

Base stations	X	Y	Z
1	86.276	104.751	32.076
2	-71.341	87.016	16.582
3	-66.469	-93.570	7.258
4	88.214	-91.227	22.854

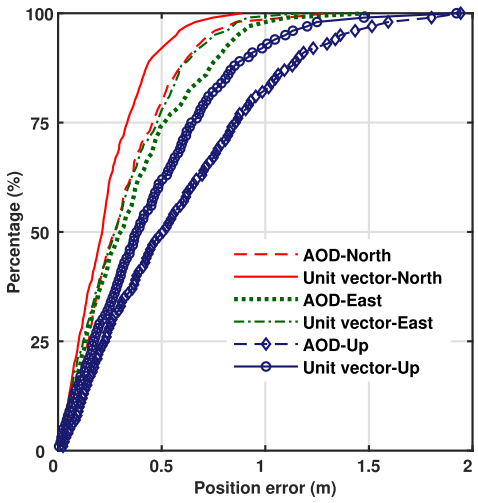

Fig. 5. Positioning results distribution of the two methods in three directions.

can maintain high positioning accuracy when the observation noise is small. And with the observation noise std is greater than 1°, the positioning effect of unit vector in three directions is better than that of AOD. When the observation noise reaches 2°, compared with AOD, the accuracy of unit vector in the three directions is improved by 18.4%, 20.5%, and 15.85%, respectively.

From the analysis results in Fig. 4, it can be concluded that the unit vector method has better positioning performance in the above-mentioned BS deployment environment. Considering that in real application scenarios, BSs are mostly deployed above UE, we simulate a new set of BS deployment schemes

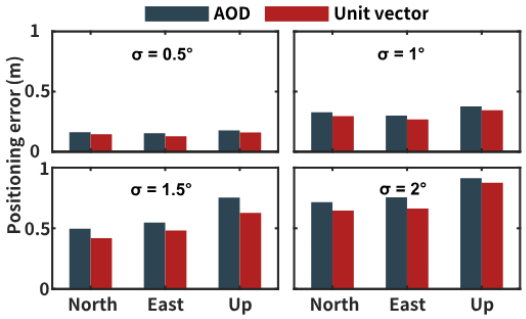

Fig. 6. 5G positioning result of AOD/unit vector.

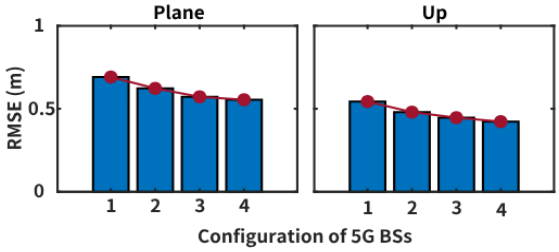

Fig. 7. Result of different configuration for the 5G system.

according to Table III, and verify the performance of the proposed method through experiments.

Taking the dataset with std of 1.5° as an example, we show the positioning results distribution of the two methods in three directions in Fig. 5. The dotted line represents the positioning result of AOD, and the solid line represents the positioning result of the unit vector. It can be clearly seen that after using the unit vector, 75% of the plane positioning results of the 5G positioning system are within 0.5 m. Compared to the AOD positioning results, 85% of the positioning results in up direction are within 1 m, and the positioning accuracy and reliability of unit vector are significantly improved. Similarly, we set up multiple groups of experiments to have better statistics, and the positioning results are shown in Fig. 6.

It can also be concluded from Fig. 6 that the effect of the unit vector method is still better than the AOD method, and as the noise std increases, the improvement effect is more obvious. Remarkably, the positioning effect in the up direction decreases in this BS deployment scenario. Hence, to further improve the positioning effect, we conduct research on the deployment height of 5G BSs.

3) For BS Height: There are four different configuration for the 5G system, which are regarded as Config. 1–4. The plane coordinates of the four configurations remain unchanged, and the heights of the BSs are different. The vertical dilution of precision (VDOP) of the various configurations are 3.845, 2.452, 1.512, and 1.139, respectively.

The localization results for four different simulated 5G configurations are presented in Fig. 7. It is not difficult to find that the positioning accuracy of Config. 1 is the worst, and the errors of plane and up are 0.691 and 0.543 m, respectively. Correspondingly, Config. 1 corresponds to the largest VDOP, when the VDOP is reduced to less than 2, the plane and up accuracy are also improved by at least 17% and 18%, respectively. These findings indicate the significance of considering the geometry of BSs height during the deployment of 5G systems.

Authorized licensed use limited to: Universitat Autonoma De Barcelona. Downloaded on January 18,2024 at 17:09:47 UTC from IEEE Xplore. Restrictions apply.

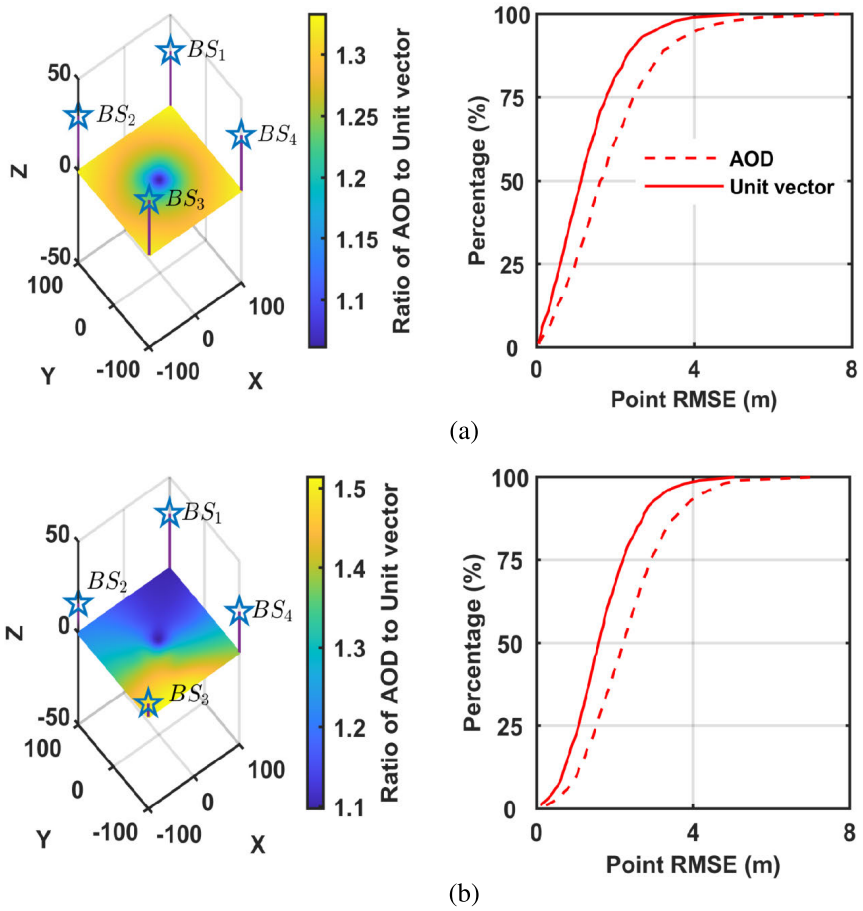

Fig. 8. Performance comparison of the AOD and Unit vector under different BS height schemes and different UE locations. (a) Result of different UE's locations in the 5G system within the same BSs height. (b) Result of different UE's locations in the 5G system within the different BSs height.

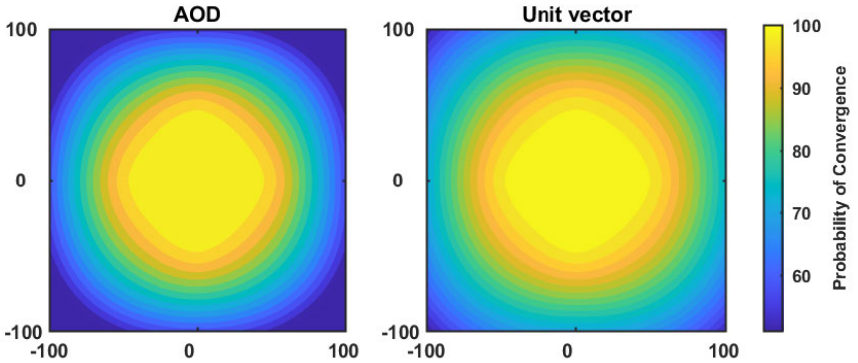

Fig. 9. Convergence performance of two methods positioning under different initial coordinates. The convergence condition is that the point error is less than twice the CRLB (3 m).

In addition, we also evaluate the performance of the two methods under different UE locations. Among them, the distance between adjacent BSs is set to 200 m, and ratio is the positioning result of AOD divided the positioning result of unit vector. Fig. 8(a) shows the solution accuracy provided by the two methods under different UE coordinates, and all BSs are placed at the same height. The left panel of Fig. 8(a) shows the ratio in point errors between the two methods at different locations. It proves that in this scenario, the positioning effect of the unit vector is better than the AOD method, and as the user continues to move to the edge, the advantages of the unit vector method are more prominent. The right panel of Fig. 8(a) shows the cumulative distribution function (cdf) of the positioning results of all test points in this area. It can be clearly seen that more than 80% of the point errors in the unit vector method is within 2 m, and the positioning stability has been significantly improved.

Fig. 8(b) shows the performance comparison of the two methods under different BS placement heights. The same conclusion as that in Fig. 8(a) can be obtained through analysis, which further proves the feasibility of the unit vector method. It is worth noting that in Fig. 8(b), the ratio distribution of the two methods is not uniform, which is caused by the different heights of the BSs.

Considering that the initial coordinates will also affect the positioning effect, we compared the positioning performance

Authorized licensed use limited to: Universitat Autonoma De Barcelona. Downloaded on January 18,2024 at 17:09:47 UTC from IEEE Xplore. Restrictions apply.

Fig. 10. Schematic of the data collection point and its surrounding environment.

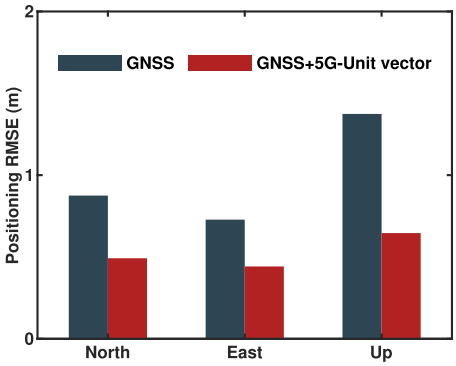

Fig. 11. Positioning result of GNSS and GNSS + 5G.

of the two methods under different initial coordinates. It can be concluded from Fig. 9 that when the initial coordinates are close to the real coordinates, the convergence probabilities of both methods reach more than 95%, and the convergence probabilities gradually decrease as the initial deviation increases. When the initial error reaches 100 m, the convergence probability of the AOD method has been reduced to 65.6%, while the convergence probability of the unit vector method is 74.2%.

B. GNSS + 5G Simulation Experiment

The GNSS observation dataset were collected by HUAWEI P40 smartphone at the Southeast University Jiulonghu Campus on Day 217 of 2022. The HUAWEI P40 is equipped with the Kirin990 5G chipset, and it supports tracking GPS (L1/L5), GALILEO (E1/E5a), BDS (B1), and GLONASS (G1) satellite signals. The sampling rate is 1 s.

Fig. 10 shows the surrounding environment of the data collection point, and it can be seen that there are tall buildings around, which will seriously affect the quality of smartphone observation, resulting in a decrease in positioning accuracy. To improve the positioning effect, we integrate 5G signals with GNSS for positioning. Considering the surrounding observation environment, the observation noise std of the 5G simulation data is set to 1.5°.

We present the GNSS positioning results and GNSS + 5G positioning results in Fig. 11. From the figure, we can find that the positioning result of GNSS is not ideal, the plane positioning error is 1.138 m, and the positioning error in the up direction is 1.374 m. After adding 5G observations, the positioning errors in the north, east, and up directions are 0.492, 0.442, and 0.646 m, the improvement effects have reached 43.7%, 38.3%, and 52.9%, respectively.

TABLE IV
RMSE OF THE POSITIONING ERROR FOR GNSS AND GNSS/5G

	GNSS	GNSS/5G-TOA	GNSS/5G-Unit vector	Improvement
N	1.354	0.954	0.485	49.20%
E	1.169	0.917	0.447	51.30%
U	1.526	1.349	0.682	49.40%

Note: The improvement refers to the improvement effect of the GNSS/5G-Unit vector model compared to the GNSS/5G-TOA model.

Furthermore, we collected another dataset at the location shown in Fig. 10 on Day 263 of 2022, to compare the effects of the TOA and the unit vector method with GNSS hybrid positioning. And the observation noise STD of the 5G simulation TOA and unit vector method are 0.3 m and 1.5°, respectively. The positioning errors in the horizontal and vertical directions of the two methods are shown in Fig. 12, where the left panel is the scatters of the horizontal error, and the right panel is the cdf of the vertical error. In the left panel, the blue scatters represent the GNSS + 5G-TOA results, the yellow scatters represent the GNSS + 5G-Unit vector results, and we also added the confidence ellipse in the left panel for comparing the effect (GNSS + 5G-TOA is in red, and the GNSS + 5G-Unit vector is in green).The results readily reveals that GNSS + 5G-Unit vector exhibits significantly superior reliability and accuracy. And it can be concluded from the right panel in Fig. 12 that the positioning accuracy is improved more obviously after using unit-vector and numerical results are displayed in Table IV. The 95% level of positioning error in the vertical component is displayed in right panel, and 95th percentile of the error decreases from 1.752 to 0.953 m.

IV. CONCLUSION

In this study, we introduced a novel 5G observation model and developed a GNSS and 5G hybrid positioning algorithm based on it, with its performance verified through experiments. Our approach involves several key steps, which we summarize as follows.

1) We have conducted an analysis of the advantages of utilizing 5G mmWave in the hybrid positioning system and delve into research on the AOD model. To address linearization errors, we proposed an observation model based on unit vectors and compared it through simulation experiments with the traditional AOD model. Remarkably, our unit vector observation model exhibits lower nonlinearity and is less affected by linearization errors, leading to significant improvements in the 5G system's positioning performance, especially as the noise in 5G observation data increases.
2) We investigated the layout height of 5G BSs and identify its impact on positioning performance. Specifically, the VDOP between 5G BSs influences positioning accuracy, and a suboptimal geometric structure results in increased positioning errors. Therefore, it is crucial to consider this factor when configuring a 5G positioning system.
3) Addressing the challenges of urban environments, where building interference decreases the reliability of smartphone GNSS positioning, we proposed a GNSS + 5G

Authorized licensed use limited to: Universitat Autonoma De Barcelona. Downloaded on January 18,2024 at 17:09:47 UTC from IEEE Xplore. Restrictions apply.

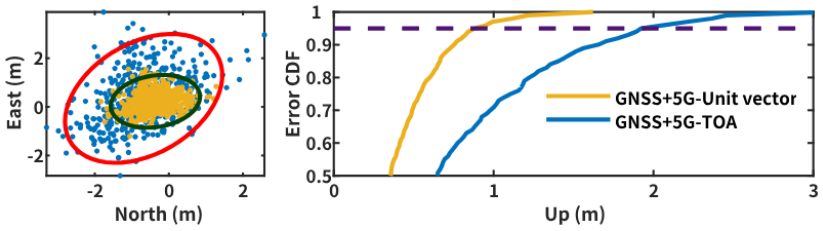

Fig. 12. Positioning results of GNSS + 5G with different methods (left panel: plane result, right panel: elevation result).

hybrid positioning model. The results showed significant improvements in positioning accuracy, even in occluded environments, providing decimeter-level navigation solutions. Consequently, our proposed model offers valuable insights for seamless indoor and outdoor positioning system research.

In conclusion, our study demonstrates the potential of the GNSS + 5G hybrid positioning model in enhancing position accuracy and reliability. It can be utilized in the development of seamless positioning systems for various applications. Looking ahead, future research should focus on developing appropriate GNSS + 5G hybrid positioning algorithms for dynamic environments and exploring solutions to address nonline-of-sight signals during 5G signal propagation. These advancements will further enhance the practicality and effectiveness of the proposed model in real-world scenarios.

ACKNOWLEDGMENT

The authors would like to thank the editors and reviewers for their comments and suggestions.

REFERENCES

[1] R. Silva and R. Iqbal, "Ethical implications of social Internet of Vehicles systems," *IEEE Internet Things J.*, vol. 6, no. 1, pp. 517–531, Feb. 2019.

[2] M. M. Rana, "IoT-based electric vehicle state estimation and control algorithms under cyber attacks," *IEEE Internet Things J.*, vol. 7, no. 2, pp. 874–881, Feb. 2020.

[3] R. Shang, C. Gao, L. Gan, R. Zhang, W. Gao, and X. Meng, "Multi-GNSS differential inter-system bias estimation for smartphone RTK positioning: Feasibility analysis and performance," *Remote Sens.*, vol. 15, no. 6, p. 1476, Mar. 2023.

[4] F. Zangenehnejad and Y. Gao, "GNSS smartphones positioning: Advances, challenges, opportunities, and future perspectives," *Satell. Navigat.*, vol. 2, no. 1, pp. 1–23, Nov. 2021.

[5] C. Jiang et al., "Smartphone PDR/GNSS integration via factor graph optimization for pedestrian navigation," *IEEE Trans. Instrum. Meas.*, vol. 71, pp. 1–12, 2022.

[6] J. Paziewski, M. Fortunato, A. Mazzoni, and R. Odolinski, "An analysis of multi-GNSS observations tracked by recent Android smartphones and smartphone-only relative positioning results," *Measurement*, vol. 175, Apr. 2021, Art. no. 109162.

[7] L. Wanninger and A. Heßelbarth, "GNSS code and carrier phase observations of a huawei P30 smartphone: Quality assessment and centimeter-accurate positioning," *GPS Solutions*, vol. 24, no. 2, p. 64, Apr. 2020.

[8] H. Yuan, Z. Zhang, X. He, Y. Wen, and J. Zeng, "An extended robust estimation method considering the multipath effects in GNSS real-time kinematic positioning," *IEEE Trans. Instrum. Meas.*, vol. 71, pp. 1–9, 2022.

[9] G. Shinghal and S. Bisnath, "Analysis and pre-processing of raw measurements from smartphones in realistic environments," in *Proc. 33rd Int. Tech. Meeting Satell. Division Inst. Navigat. (ION GNSS+)*, Oct. 2020, pp. 3140–3154.

[10] J. del Peral-Rosado, J. Saloranta, G. Destino, J. López-Salcedo, and G. Seco-Granados, "Methodology for simulating 5G and GNSS high-accuracy positioning," *Sensors*, vol. 18, no. 10, p. 3220, Sep. 2018.

[11] J. A. del Peral-Rosado, R. Raulefs, J. A. López-Salcedo, and G. Seco-Granados, "Survey of cellular mobile radio localization methods: From 1G to 5G," *IEEE Commun. Surveys Tuts.*, vol. 20, no. 2, pp. 1124–1148, 2nd Quart., 2018.

[12] H. Maluleke, A. Bagula, O. Ajayi, and L. Chiaraviglio, "An economic feasibility model for sustainable 5G networks in rural dwellings of south Africa," *Sustainability*, vol. 14, no. 19, p. 12153, Sep. 2022.

[13] P. Minango, Y. Iano, E. L. Chuma, G. C. Vaz, G. G. de Oliveira, and J. Minango, "Revision of the 5G concept rollout and its application in smart cities: A study case in South America," in *Proc. Brazilian Technol. Symp.* Campinas, Brazil: Springer, 2021, pp. 229–238.

[14] S. Forge and K. Vu, "Forming a 5G strategy for developing countries: A note for policy makers," *Telecommun. Policy*, vol. 44, no. 7, Aug. 2020, Art. no. 101975.

[15] I. A. Lami, H. S. Maghdid, and T. Kuseler, "SILS: A smart indoors localisation scheme based on on-the-go cooperative smartphones networks using onboard bluetooth, WiFi and GNSS," in *Proc. 27th Int. Tech. Meeting Satell. Division Inst. Navigat. (ION GNSS)*, 2014, pp. 503–509.

[16] Y. Gao, X. Meng, C. M. Hancock, S. Stephenson, and Q. Zhang, "UWB/GNSS-based cooperative positioning method for V2X applications," in *Proc. 27th Int. Tech. Meeting Satell. Division Inst. Navigat. (ION GNSS)*, 2014, pp. 3212–3221.

[17] Y. Du and D. Yang, "Seamless positioning and navigation system based on GNSS, WiFi and PDR for mobile devices," in *Proc. 1st EAI Int. Conf. Artif. Intell. Commun. Netw. (AICON)*. Harbin, China: Springer, May 2019, pp. 522–540.

[18] K.-W. Chiang et al., "Semantic proximity update of GNSS/INS/VINS for seamless vehicular navigation using smartphone sensors," *IEEE Internet Things J.*, vol. 10, no. 17, pp. 15736–15748, Sep. 2023.

[19] C. Jiang et al., "Implementation and performance analysis of the PDR/GNSS integration on a smartphone," *GPS Solutions*, vol. 26, no. 3, p. 81, Jul. 2022.

[20] L. Mailaender, "Comparing geo-location bounds for TOA, TDOA, and round-trip toa," in *Proc. IEEE 18th Int. Symp. Pers., Indoor Mobile Radio Commun.*, Sep. 2007, pp. 1–5.

[21] C. Jin, W. P. Tay, K. Zhao, K. V. Ling, and K. K. Sin, "A 5G/GNSS integrated positioning method," in *Proc. Int. Tech. Meeting Satell. Division Inst. Navigat. (ION GNSS)*, Oct. 2022, pp. 2429–2443.

[22] M. Ahadi and F. Kaltenberger, "5GNR indoor positioning by joint DL-TDoA and DL-AoD," in *Proc. IEEE Wireless Commun. Netw. Conf. (WCNC)*, Mar. 2023, pp. 1–6.

[23] S. Sosnin, A. Lomayev, and A. Khoryaev, "DL-AOD positioning algorithm for enhanced 5G NR location services," in *Proc. Int. Conf. Indoor Positioning Indoor Navigat. (IPIN)*, Nov. 2021, pp. 1–7.

[24] X. Wei, N. Palleit, and T. Weber, "AOD/AOA/TOA-based 3D positioning in NLOS multipath environments," in *Proc. IEEE 22nd Int. Symp. Pers., Indoor Mobile Radio Commun.*, Sep. 2011, pp. 1289–1293.

[25] M. Alghisi and L. Biagi, "Positioning with GNSS and 5G: Analysis of geometric accuracy in urban scenarios," *Sensors*, vol. 23, no. 4, p. 2181, Feb. 2023. [Online]. Available: https://www.mdpi.com/1424-8220/23/4/2181

[26] W. Zhang, Y. Yang, A. Zeng, and Y. Xu, "A GNSS/5G integrated three-dimensional positioning scheme based on D2D communication," *Remote Sens.*, vol. 14, no. 6, p. 1517, Mar. 2022. [Online]. Available: https://www.mdpi.com/2072-4292/14/6/1517

[27] J. A. del Peral-Rosado et al., "Physical-layer abstraction for hybrid GNSS and 5G positioning evaluations," in *Proc. IEEE 90th Veh. Technol. Conf. (VTC-Fall)*, Sep. 2019, pp. 1–6.

[28] J. A. del Peral-Rosado et al., "Exploitation of 3D city maps for hybrid 5G RTT and GNSS positioning simulations," in *Proc. IEEE Int. Conf. Acoust., Speech Signal Process. (ICASSP)*, May 2020, pp. 9205–9209.

Authorized licensed use limited to: Universitat Autonoma De Barcelona. Downloaded on January 18,2024 at 17:09:47 UTC from IEEE Xplore. Restrictions apply.

[29] F. Li, R. Tu, J. Hong, S. Zhang, P. Zhang, and X. Lu, "Combined positioning algorithm based on BeiDou navigation satellite system and raw 5G observations," *Measurement*, vol. 190, Feb. 2022, Art. no. 110763.
[30] C. Sun, H. Zhao, L. Bai, J. W. Cheong, A. G. Dempster, and W. Feng, "GNSS-5G hybrid positioning based on TOA/AOA measurements," in *Proc. China Satell. Navigat. Conf. (CSNC)*, vol. 3. Chengdu, China: Springer, 2020, pp. 527–537.
[31] J. Huang, J. Liang, and S. Luo, "Method and analysis of TOA-based localization in 5G ultra-dense networks with randomly distributed nodes," *IEEE Access*, vol. 7, pp. 174986–175002, 2019.
[32] R. B. Langley, "GPS receiver system noise," *GPS World*, vol. 8, no. 6, pp. 40–45, 1997.
[33] N. Cressie, "Fitting variogram models by weighted least squares," *J. Int. Assoc. Math. Geol.*, vol. 17, no. 5, pp. 563–586, Jul. 1985.
[34] *5G NR: Physical Channels and Modulation*, document TS 38.211, Rel. 16, 3GPP, Sophia Antipolis, 2018.
[35] L. S. Pillutla and R. Annavajjala, "CRLB calculations for joint AoA, AoD and multipath gain estimation in millimeter wave wireless networks," 2017, *arXiv:1704.00453*.

Qi Liu is currently pursuing the Ph.D. degree with the School of Transportation, Southeast University, Nanjing, China.

His current research interests include multisensor integration, high-precision positioning of smartphones in challenging environments, and positioning with 5G.

Chengfa Gao received the Ph.D. degree from Southeast University, Nanjing, China, in 2004.

He is currently a Professor with the School of Transportation, Southeast University. His current research interests include GNSS high-precision navigation and positioning theory and engineering application research, and multisource position information processing theory for the general public.

Alda Xhafa received the B.Sc. degree in telecommunication engineering from the Polytechnic University of Tirana (UPT), Tirana, Albania, in 2015, and the M.Sc. degree in telecommunication engineering from the Universitat Politecnica de Catalunya (UPC), Barcelona, Spain, in 2017. She is currently pursuing the Ph.D. degree with the Universitat Autonoma de Barcelona (UAB), Bellaterra, Spain.

From March 2018 to September 2019, she was an Assistant Lecturer with the Department of Electronics and Telecommunications, Faculty of Information Technology, UPT. Her research interests are in wireless communications, terrestrial localization systems, and positioning with 5G technologies.

Wang Gao received the Ph.D. degree from the School of Transportation, Southeast University, Nanjing, China, in 2018.

He is currently an Associate Professor with the School of Instrument Science and Engineering, Southeast University. His current research interests include multisystem and multifrequency GNSS integer ambiguity resolution and high-precision positioning.

José A. López-Salcedo (Senior Member, IEEE) received the M.Sc. and Ph.D. degrees in telecommunication engineering from the Universitat Politècnica de Catalunya, Barcelona, Spain, in 2001 and 2007, respectively.

Since 2006, he has been with the Universitat Autònoma de Barcelona, Bellaterra, Spain, where he is currently a Professor, and served as a Coordinator of the Telecommunications Engineering degree from 2011 to 2019. He is also with the Institute of Spatial Studies of Catalonia (IEEC) and the Co-Founder of the startup company Loctio. He has held several visiting appointments with the University of Illinois Urbana–Champaign, Champaign, IL, USA, the University of California at Irvine, Irvine, CA, USA, and the European Commission Joint Research Center. He has been the Principal Investigator of more than 25 research projects, most of them funded by the European Space Agency (ESA) on topics dealing with signal processing for GNSS receivers. His research interests include signal processing for communications and navigation, with emphasis on the convergence between GNSS, 5G/6G and LEO satellites for Positioning, Navigation, and Timing (PNT).

Dr. López-Salcedo serves as a Secretary and Treasurer of the Spanish Chapter of the IEEE Aerospace and Electronic Systems Society (AESS), a member of the Editorial Committee of the Korean Institute of Positioning, Navigation and Timing (IPNT), and a member of the IEEE Signal Processing Society Sensor Array and Multichannel Technical Committee (SAM TC).

Gonzalo Seco-Granados (Fellow, IEEE) received the Ph.D. degree in telecommunications engineering from the Universitat Politècnica de Catalunya, Barcelona, Spain, in 2000, and the M.B.A. degree from the IESE Business School, Barcelona, in 2002.

From 2002 to 2005, he was a member of the European Space Agency, Madrid, Spain, where he was involved in the design of the Galileo system. He is currently a Professor with the Department of Telecommunication, Universitat Autònoma de Barcelona, Bellaterra, Spain, where he served as the Coordinator of the Telecommunications Engineering degree, from 2007 to 2010 and the Vice Dean of the Engineering School, from 2011 to 2019. In 2015, 2019, and 2022, he was a Fulbright Visiting Scholar with the University of California at Irvine, Irvine, CA, USA. He is also with the Institute of Spatial Studies of Catalonia (IEEC) and a ICREA Academia fellow. He is a Co-Founder of Loctio, a startup providing low-energy GNSS positioning solutions for IoT. He has more than 370 publications in his research areas and holds five related patents. His research interests include GNSS, and beyond 5G integrated communications, localization, and sensing.

Dr. Seco-Granados serves as a member of the IEEE Signal Processing Society Sensor Array and Multichannel Technical Committee (SAM TC), and the EURASIP Signal Processing for Multisensor Systems Technical Committee, since 2018 and 2022, respectively. Since 2019, he has been a President of the Spanish Chapter of the IEEE Aerospace and Electronic Systems Society. He received the IEEE Signal Processing Society's Best Paper Award in 2021.

Authorized licensed use limited to: Universitat Autonoma De Barcelona. Downloaded on January 18,2024 at 17:09:47 UTC from IEEE Xplore. Restrictions apply.